Stem Cell Reports
Report

ISSCR

OPEN ACCESS

Development of Gonadotropin-Releasing Hormone-Secreting Neurons from Human Pluripotent Stem Cells

Carina Lund,[1] Kristiina Pulli,[1] Venkatram Yellapragada,[1] Paolo Giacobini,[3,4] Karolina Lundin,[5] Sanna Vuoristo,[1] Timo Tuuri,[5] Parinya Noisa,[6,7,8] and Taneli Raivio[1,2,7,8,*]

[1]Faculty of Medicine, Department of Physiology, University of Helsinki, Helsinki 00014, Finland
[2]Children's Hospital, Pediatric Research Center, Helsinki University Central Hospital (HUCH), Helsinki 00029, Finland
[3]Inserm, Jean-Pierre Aubert Research Center, Development and Plasticity of the Neuroendocrine Brain, Unité 1172, 59045 Lille Cedex, France
[4]School of Medicine, University of Lille, Lille 59000, France
[5]Department of Obstetrics and Gynecology, HUCH, Helsinki 00029, Finland
[6]School of Biotechnology, Institute of Agricultural Technology, Suranaree University of Technology, Nakhon Ratchasima 30000, Thailand
[7]Faculty of Medicine/Physiology, University of Helsinki, Biomedicum Helsinki, PO Box 63 (Haartmaninkatu 8), Helsinki 00014, Finland
[8]Co-senior author
*Correspondence: taneli.raivio@helsinki.fi
http://dx.doi.org/10.1016/j.stemcr.2016.06.007

SUMMARY

Gonadotropin-releasing hormone (GnRH) neurons regulate human puberty and reproduction. Modeling their development and function in vitro would be of interest for both basic research and clinical translation. Here, we report a three-step protocol to differentiate human pluripotent stem cells (hPSCs) into GnRH-secreting neurons. Firstly, hPSCs were differentiated to *FOXG1*, *EMX2*, and *PAX6* expressing anterior neural progenitor cells (NPCs) by dual SMAD inhibition. Secondly, NPCs were treated for 10 days with FGF8, which is a key ligand implicated in GnRH neuron ontogeny, and finally, the cells were matured with Notch inhibitor to bipolar TUJ1-positive neurons that robustly expressed *GNRH1* and secreted GnRH decapeptide into the culture medium. The protocol was reproducible both in human embryonic stem cells and induced pluripotent stem cells, and thus provides a translational tool for investigating the mechanisms of human puberty and its disorders.

INTRODUCTION

The onset of puberty is regulated by a small population of hypothalamic gonadotropin-releasing hormone (GnRH) neurons, which secrete GnRH decapeptide to the hypophyseal portal system. Unlike other neuroendocrine cell types that reside in the hypothalamus, GnRH neurons are born outside the CNS in the frontonasal area. The olfactory pit, which is formed by the olfactory placodes (OP) and surrounding mesenchyme, provides a niche for GnRH neuron specification. Prenatally, GnRH neurons migrate from the frontonasal mesenchyme along with olfactory axons to the forebrain and into the hypothalamus, where their final maturation occurs (Wray, 2010). The early events that lead to GnRH neuron specification and the origin of their progenitors in the olfactory pit are currently poorly understood. Many existing data support OP as the source of GnRH neurons (Kim et al., 1999; Schwanzel-Fukuda and Pfaff, 1989; Wray et al., 1989a, 1989b), whereas others have proposed that at least some GnRH neurons arise from multiple sources, such as the neural crest, and adenohypophyseal or CNS progenitor cells (Forni et al., 2011; Markakis et al., 2004; Salvi et al., 2009; Whitlock et al., 2003).

GnRH neuron specification occurs under explicit spatiotemporal conditions, involving fibroblast growth factor 8 (FGF8) signaling and bone morphogenetic protein/transforming growth factor β (BMP/TGF-β) pathway inhibition (Forni et al., 2013; Kawauchi et al., 2005; Rawson et al., 2010). The indispensable role of FGF8 signaling through fibroblast growth factor receptor 1 (FGFR1) in this process has been established in various animal models (Chung and Tsai, 2010; Sabado et al., 2012). These findings are mirrored by reports in humans: mutations in *FGF8* and *FGFR1* are found in patients with congenital hypogonadotropic hypogonadism, a rare genetic disease that causes GnRH deficiency (Dode et al., 2003; Falardeau et al., 2008).

Human pluripotent stem cells (hPSCs), including embryonic stem cells (hESCs) and induced pluripotent stem cells (hiPSCs), allow in vitro differentiation of specialized cell types, including neurons (Chambers et al., 2009; Davis et al., 2012; Hay et al., 2008). Here we report a protocol for the generation of GnRH-expressing neurons from hPSCs.

RESULTS

A schematic of the protocol is presented in Figure 1A. In the first step, we employed dual SMAD inhibition on hPSCs by blocking BMP and TGF-β/activin signaling pathways with dorsomorphin (DM) and SB431542 (SB), respectively, for 10 days to produce neural progenitor cells (NPCs) (Chambers et al., 2009). This was followed by 10-day treatment with FGF8, a key ligand in GnRH neuron development, and 4–8 days of treatment with both FGF8 and

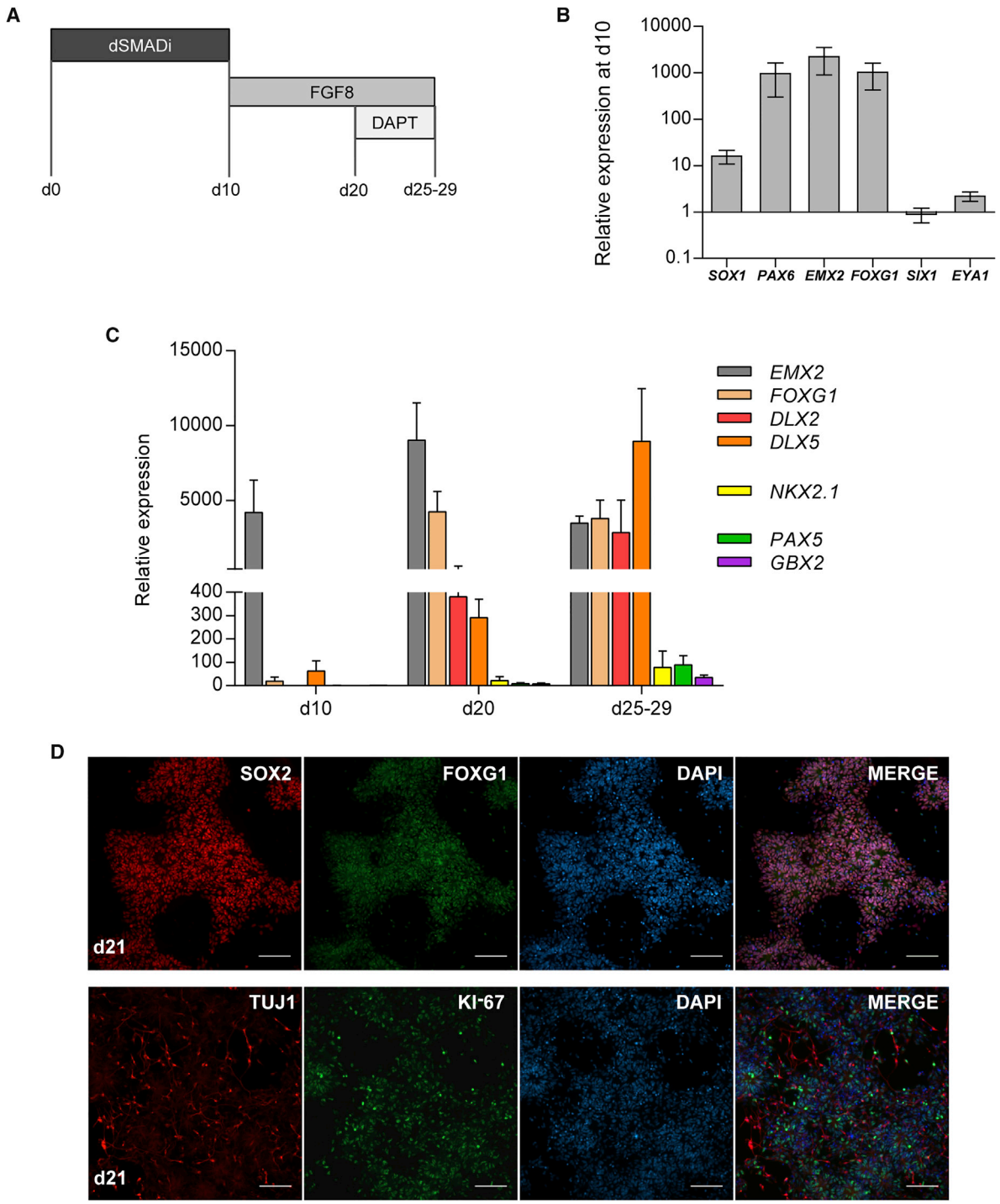

Figure 1. Differentiation Protocol Schematic, and Expression of Anterior Neural Progenitor Markers after Neural Induction

(A) Schematic representation of the protocol. For the first 10 days the cells were treated with dual SMAD inhibition (dSMADi) using dorsomorphin and SB431542. FGF8 was added at d11, and Notch inhibitor DAPT was added at d21.

(B) Real-time qPCR results at d10 showing an increased expression of pan-neural marker *SOX1* and forebrain- and olfactory placode-associated genes *EMX2* and *FOXG1*. Preplacodal markers *SIX1* and *EYA1* remained low. Expression levels are relative to d0 hPSCs (HEL11.4 and H9 representative experiments, n = 6, mean ± SEM).

(legend continued on next page)

Notch inhibitor DAPT (N-[N-(3,5-difluorophenacetyl)-L-alanyl]-S-phenylglycine t-butyl ester), to induce terminal maturation of the neurons (Borghese et al., 2010). We used hiPSC line HEL11.4 (Mikkola et al., 2013), and hESC line H9 (Thomson et al., 1998; WiCell) for differentiation experiments, and the main results were repeated in hiPSC line HEL24.3 (Trokovic et al., 2015). Both hiPSC lines have been established from healthy donor fibroblasts.

Dual SMAD Inhibition Followed by FGF8 Treatment Produces Highly Proliferating Neural Progenitor Cells that Retain Anterior Identity

Ten days of dual SMAD inhibition induced early pan-neural marker *SOX1* and neural progenitor markers *PAX6*, *EMX2*, and *FOXG1* (Figure 1B), which are expressed in the developing forebrain and the OP (Duggan et al., 2008; Forni et al., 2011; Simeone et al., 1992; Zhang et al., 2010). In contrast, the expression of preplacodal genes *EYA1* and *SIX1* (Ikeda et al., 2007; Schlosser et al., 2008) remained low (Figure 1B). Immunocytochemical analyses confirmed the expression of neural progenitor markers including PAX6, FOXG1, and SOX2, whereas preplacodal marker SIX1 was undetectable (Figure S1A). The expression levels of ventral forebrain marker *NKX2.1* and caudal markers *PAX5* and *GBX2* (Kirkeby et al., 2012; Maroof et al., 2013) were low (Figures 1C and S1B). These results indicate that dual SMAD inhibition with DM and SB for 10 days efficiently induces anteriorly patterned NPCs.

During the subsequent 10 days, the anteriorly primed NPCs were treated with FGF8. At day 20 (d20), FGF8-treated cells had further increased the expression of *EMX2* and *FOXG1*, as well as *DLX2* and *DLX5*, which are also anteriorly expressed; in the frontonasal area, the OP, and the anterior basal forebrain (Merlo et al., 2007; Simeone et al., 1994) (Figures 1C and S1B). A high expression of these anterior markers was sustained throughout the protocol, whereas the expressions of *NKX2.1*, *PAX5*, and *GBX2* remained low (Figures 1C and S1B). Between d10 and d20, the cells formed neural rosettes that abundantly expressed both SOX2 and FOXG1 (Figure 1D). Overall, an average of 93% (±0.9%, n = 5) of cells were FOXG1 positive at d21. FGF8-treated cells expanded more rapidly than the controls (Figure S1C). Proliferation occurred predominantly in the rosette structures, as judged by abundant Ki-67 expression (Figure 1D). Neural-specific TUJ1-positive cells, which were consistently negative for Ki-67, were located at the periphery and around the neural rosettes, indicating neuronal maturation and cell-cycle exit (Figure 1D).

FGF8 and Subsequent Notch Inhibition Induces GnRH Expression

To induce the terminal differentiation of NPCs, we inhibited Notch signaling with DAPT from d21 onward. After 4–8 days, the *GNRH1* mRNA level was highly increased in cells supplemented with FGF8, but not in the control cells (Figures 2A and S2A). Immunofluorescence showed presence of GnRH-positive cells mostly in the peripheral regions of condensed cell clusters (Figure 2Ba). The GnRH-positive cells were bipolar and expressed neural marker MAP2 (Figure 2Bb). Concurrently, the number of proliferating (Ki-67 positive) cells was low, and, importantly, no GnRH and Ki-67 double-positive cells were observed (Figure 2C). This indicates that the GnRH-positive cells had exited the cell cycle. The neural identity of the GnRH-expressing cells was further confirmed by double staining with TUJ1 (Figures 2D and S2B). A proportion of the GnRH-positive cells also expressed FOXG1 (Figure 2E). On average, 15.1% (±1.6%, n = 4) of the HEL11.4-derived cells and 12.2% (±4.2%, n = 3) of the H9-derived cells were GnRH positive.

Secretion of GnRH Decapeptide

Human GnRH is translated as a 96-amino-acid prohormone, which is processed by intracellular proteases to form the secreted decapeptide. The GnRH decapeptide was clearly detectable in the culture medium of the FGF8-treated cells, but not of the control cells from d25 onward, with the peak concentrations measured on d27 (Figures 3A and S3A). High-magnification images of GnRH immunopositive cells showed a punctate staining pattern in the majority of the cells, indicating vesicular packaging of GnRH decapeptide (Figures 3B and S3B). Activated caspase-3 (Porter and Janicke, 1999) was not present in the GnRH-positive cells (Figure 3C), suggesting that the release of GnRH was not due to cell death. FGF8-treated cells readily responded to KCl-induced depolarization by 1.97-fold higher GnRH decapeptide release (95% confidence interval, 1.62–2.31) when compared with vehicle-treated cells.

Migration of GnRH-Expressing Cells

$GABA_A$ receptor stimulation has been shown to decelerate the migration of embryonic mouse GnRH neurons (Casoni

(C) Relative expression of anterior neural progenitor (*EMX2*, *FOXG1*, *DLX2*, and *DLX5*), ventral forebrain (*NKX2.1*), and caudal CNS markers (*PAX5* and *GBX2*) in FGF8-treated cells confirming anterior neural identity. HEL11.4-derived cells, n = 3 (mean + SEM). Corresponding data from H9-derived cells are shown in Figure S1B.

(D) Immunocytochemistry at d21 revealed an abundant expression of SOX2, FOXG1, and Ki-67 within neural rosettes. TUJ1 was found mainly outside the neural rosette structures. HEL11.4-derived cells. Scale bars, 100 μm.

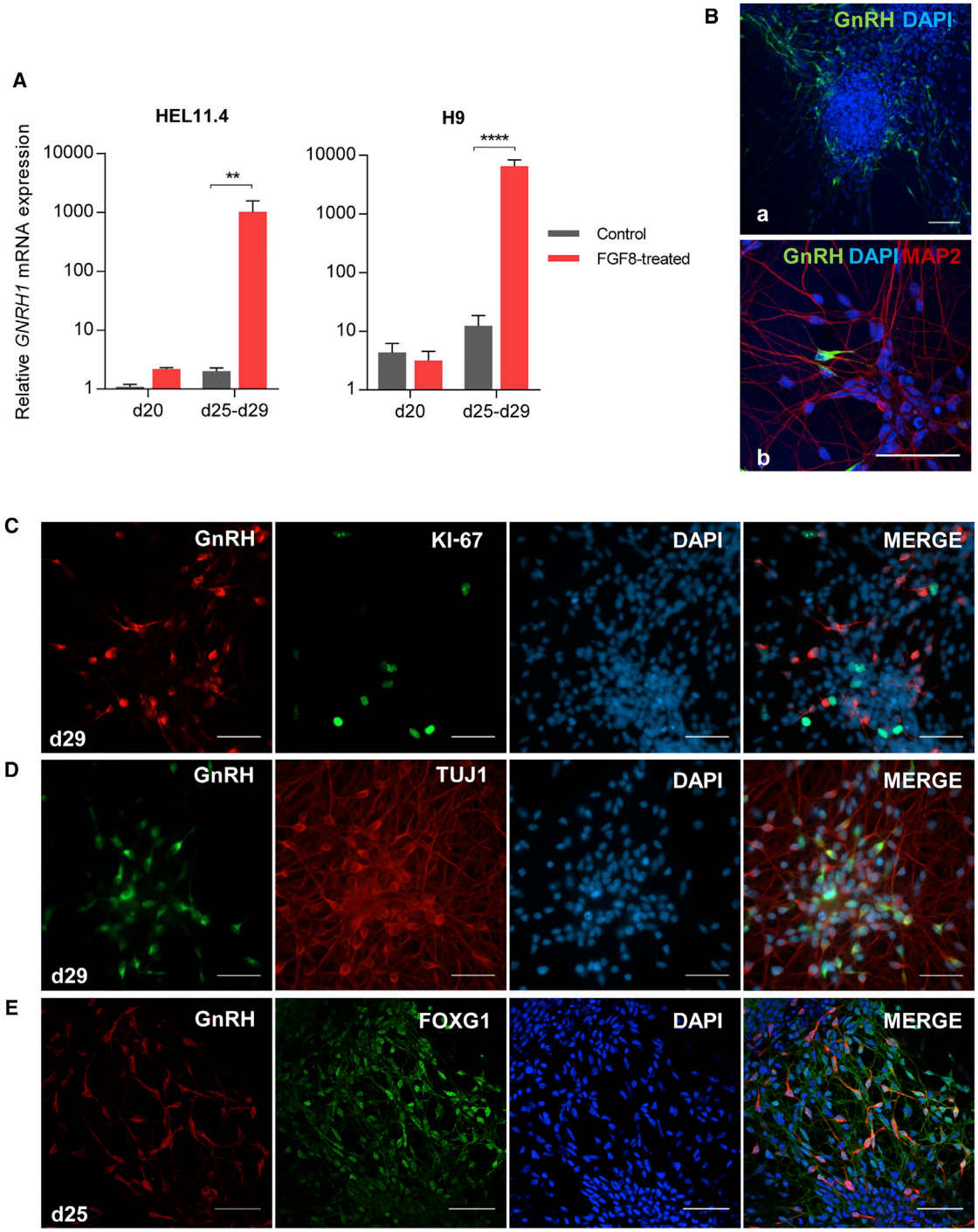

Figure 2. GnRH-Expressing Cells Emerge after Treatment with FGF8 and DAPT

(A) Relative expression of *GNRH1* at the end of the protocol in HEL11.4-derived cells (n = 4), and H9-derived cells (n = 6) treated with or without FGF8 (mean + SEM). **p < 0.01, ****p < 0.0001 (paired ratio t test).

(B–E) Immunocytochemistry in HEL11.4-derived cells at the end of the protocol. (B) GnRH-positive neurons appeared mostly in the periphery of condensed node-like structures. These cells appeared to be interconnected by long cellular projections (a), which stained positive for MAP2 (b). (C) The GnRH-expressing cells were not proliferating, as indicated by the absence of colocalization with Ki-67 staining. (D) The GnRH-positive cells also expressed neuron-specific marker TUJ1. See also Figure S2B. (E) At the end of the protocol, the majority of the cells expressed FOXG1. Some of the GnRH-positive cells were also FOXG1 positive. All scale bars represent 50 μm.

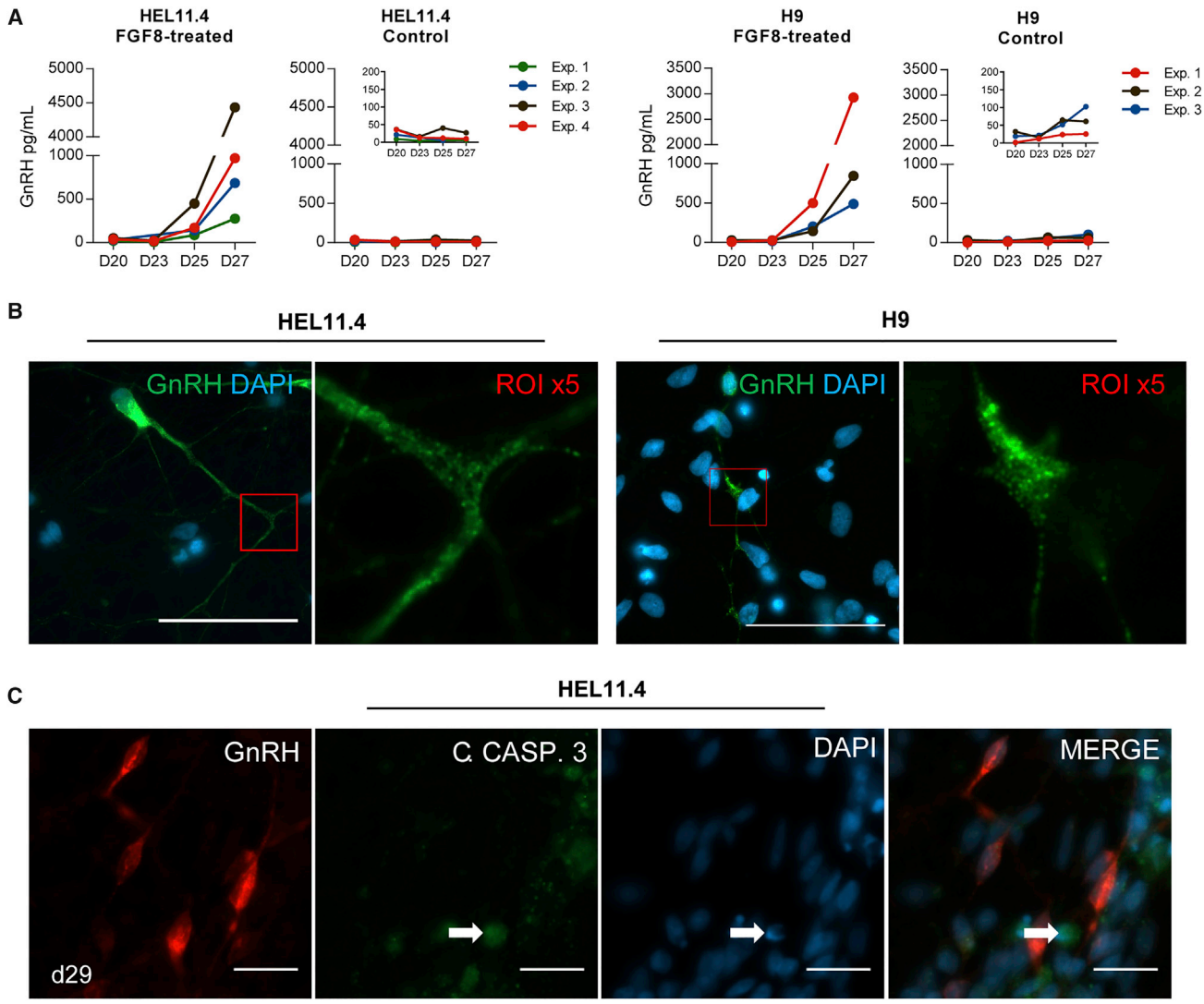

Figure 3. GnRH Decapeptide Secretion in Culture Medium of FGF8-Treated Cells

In the final differentiation step, secretion of GnRH decapeptide was detected in the culture medium of FGF8-treated cells, but not of the control cells.

(A) Four independent experiments using HEL11.4-derived cells (left) and three independent experiments from H9-derived cells (right) are shown. The insets in the control graphs show the same control values with smaller y-axis scale. See also Figure S3A.

(B) At high magnification the GnRH staining appeared in granular spots in both HEL11.4- and H9-derived cells, indicating vesicular packaging of the decapeptide. ROI, region of interest. Scale bars, 50 μm. See also Figure S3B.

(C) GnRH and an apoptosis marker, cleaved caspase-3, were not co-expressed, suggesting that GnRH-release was not due to apoptosis. HEL11.4-derived GnRH-expressing cells display normal nuclear morphology. Arrows indicate cleaved caspase-3 staining and nuclear morphology of apoptotic cell. Scale bars, 20 μm.

et al., 2012). Therefore, we investigated the migratory properties of our FGF8-treated cells with a gap-closure assay, whereby d25 cells were allowed to migrate to an empty area in the middle of the culture wells in the presence or absence of $GABA_A$ receptor agonist muscimol (0.1 mM). After 50 hr, significantly fewer cells had migrated to the empty area in muscimol-treated wells than in control wells (paired ratio t test, $n = 4$; $p < 0.05$).

Detection of GnRH-Expressing Neurons in FOXG1-Positive Frontonasal Tissues

As some GnRH cells were positive for FOXG1 in vitro, we investigated whether GnRH neurons express FOXG1 also in vivo. Immunohistochemistry on an 8-gestational-week human fetus showed migrating GnRH neurons that appeared in typical cell clusters, called the migratory mass (Miller et al., 2010; Tarozzo et al., 1995; Wray et al.,

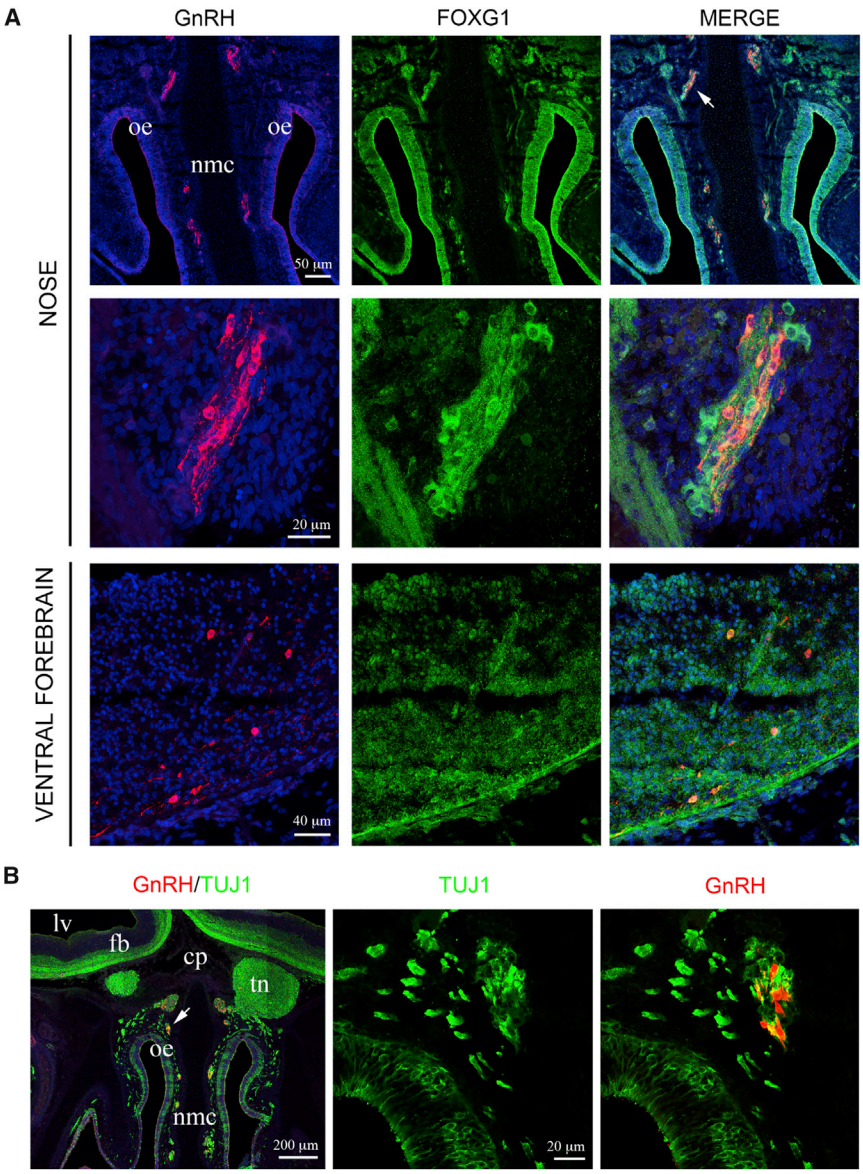

Figure 4. GnRH, FOXG1, and TUJ1 in an 8-Gestational-Week Human Fetus

(A) Immunohistochemistry of coronal sections in a human fetus. GnRH was expressed in the frontonasal area between the olfactory epithelia (oe) and the nasal medial cartilage (nmc), in migrating cells also known as the migratory mass. These cells were FOXG1-positive, including GnRH-expressing cells. The arrow in the top panel indicates the area magnified in the middle panel. GnRH-FOXG1 double-positive cells were also detected in the ventral forebrain. (B) TUJ1 was expressed in the migratory mass cells, including GnRH-expressing cells. Arrow indicates the area magnified on the right. cp, cribriform plate; fb, forebrain; lv, lateral ventricle; nmc, nasal medial cartilage; oe, olfactory epithelia; tn, terminal nerve.

1994). The cell clusters contained GnRH neurons, other neurons, and glial cells that delaminated from the olfactory epithelium and migrated toward the forebrain (Figure 4A). Indeed, FOXG1 was expressed in the GnRH neurons, as well as in other cells of the migratory mass and the olfactory epithelium (Figure 4A). Many GnRH-positive cells appeared also to stain with TUJ1 (Figure 4B).

DISCUSSION

According to current understanding, GnRH neurons are first formed during early embryogenesis in the olfactory placode area, from where they migrate to the hypothalamus via the vomeronasal/terminal nerve fibers (Wray, 2010). Once at their final destination, they mature and become an integral part of the hypothalamic-pituitary-gonadal axis. While the OP have been generally accepted as a source of GnRH neurons, the exact origin of GnRH neuron progenitors has remained controversial. Our results show that GnRH-secreting cells can be efficiently differentiated from NPCs that express high levels of anterior neural progenitor markers. The induction of neural commitment in hPSCs by using dual SMAD inhibition leads by default to anterior neural cell fates (Chambers et al., 2009; Kirkeby et al., 2012; Pankratz et al., 2007). Indeed, our dual SMAD inhibition-treated NPCs showed high expression of *FOXG1* and *EMX2*. Expressed in the frontonasal area, where GnRH neurons first emerge, *FOXG1*, *DLX2*, and *DLX5* have been suggested to be involved in GnRH neuron

development (Duggan et al., 2008; Givens et al., 2005; Iyer et al., 2010). Indeed, all of these markers were upregulated along our differentiation protocol. Placodal markers *SIX1* and *EYA1* (Schlosser, 2014) were, however, not upregulated at any time during this protocol.

Our results show that anterior NPCs can give rise to GnRH-expressing cells when cultured with FGF8, which has been shown to promote progenitor cell survival in the anterior neural structures (Forni et al., 2013; Kawauchi et al., 2005). In mouse anterior neural ridge, FGF8 has been shown to positively regulate *Foxg1* expression (Shimamura and Rubenstein, 1997), and mouse embryos that carry hypomorphic and conditional *Fgf8* mutations display reduced telencephalons, which is suggested to result from a decreased *Foxg1* expression (Storm et al., 2006). In our model, *FOXG1* expression persisted following FGF8 treatment, and importantly, FOXG1 was also expressed in migrating GnRH neurons of a human fetus.

The final step in our protocol comprised Notch inhibition, which induces neuronal maturation from progenitor cells (Borghese et al., 2010; Imayoshi et al., 2010; Noisa et al., 2014; Yoon and Gaiano, 2005). As expected, the blocking of Notch in our FGF8-treated cells after d20 decelerated cell proliferation, increased the expression of neuron-specific markers TUJ1 and MAP2, and induced *GNRH1* expression, with up to 15% of the cells being immunopositive for GnRH. This efficiency is high, given that humans only have few thousand GnRH neurons. Two recent publications have reported hPSC differentiation to hypothalamic-like neuroendocrine cells, such as POMC-, αMSH-, and AGRP-secreting neurons (Merkle et al., 2015; Wang et al., 2015). In both approaches, dual SMAD inhibition in combination with SHH activation led to ventral forebrain progenitor stage, as suggested by marker expression patterns including high *NKX2.1* and low *FOXG1* expression. It is noteworthy that these two protocols did not report an induction of *GNRH1* expression, which highlights the known differences in the embryonic origin of these cells. In contrast, our protocol produced GnRH-expressing cells with long cellular processes consistent with previously described morphology of GnRH neurons (Herde et al., 2013). The $GABA_A$ receptor agonist muscimol suppressed the migration of GnRH-expressing cells, in agreement with the studies performed in embryonic mouse GnRH neurons (Casoni et al., 2012). In the majority of GnRH-expressing cells the GnRH staining appeared in punctate structures, indicating GnRH prepropeptide processing to mature decapeptide and packaging into secretory vesicles. The cultures indeed robustly secreted GnRH into culture medium. Future studies are required to further characterize the neuroendocrine properties of these GnRH-expressing cells. Our protocol was reproducible in hiPSCs, which implicates that it can be employed to model diseases that affect GnRH neuron specification, such as hypogonadotropic hypogonadism due to congenital GnRH deficiency.

EXPERIMENTAL PROCEDURES

See also Supplemental Experimental Procedures.

Human Pluripotent Stem Cells

hESC line H9 ((Thomson et al., 1998); Wicell) and two hiPSC lines HEL11.4 (Mikkola et al., 2013) and HEL24.3 (Trokovic et al., 2015) were used in this study. hPSCs were maintained on Geltrex-coated plates with StemPro or Essential 8 medium.

GnRH Neuron Differentiation

N2B27 medium was used throughout the differentiation protocol. For d0–d10, medium was supplemented with dual SMAD inhibitors, 2 μM dorsomorphin, and 10 μM SB431542 (Sigma). At day 11, dual SMAD inhibition was withdrawn and 100 ng/ml FGF8 (Peprotech) was added. From d21 onward, medium was supplemented with both FGF8 and 20 μM Notch inhibitor DAPT (Sigma). Control cells did not receive FGF8 supplementation.

Analysis of GnRH Expression and Secretion

RNA extraction and real-time qPCR were performed using standard protocols. The expression levels of target genes were normalized to cyclophilin G, and compared with undifferentiated hPSCs. For immunocytochemistry, cells were fixed by 4% paraformaldehyde and immunostainings were performed using standard protocols. FOXG1 and GnRH immunopositive cells were quantified by manually counting the cells in images taken with a 40× objective. Secreted GnRH was quantified by a competitive fluorescent enzyme immunoassay.

Human Samples

A human fetus (8 gestational weeks) was obtained from a voluntarily terminated pregnancy with the parent's written informed consent. Permission to utilize human fetal tissues was obtained from the French agency for biomedical research (Agene de la Biomédecine, Saint-Denis la Plaine, France, protocol no. PFS16-002). Tissues were made available in accordance with French bylaws. Tissues were fixed with 4% paraformaldehyde and immunostaining was performed on 20-μm cryosections. Immunostaining was performed according to standard procedures (INSERM).

Statistical Analyses

When used, "n" always stands for number of independent experiments. Statistical comparisons were performed by using paired ratio t test in Prism 5.0 (GraphPad). $p < 0.05$ was accepted to indicate statistical significance.

SUPPLEMENTAL INFORMATION

Supplemental Information includes Supplemental Experimental Procedures, three figures, and two tables and can be found with this article online at http://dx.doi.org/10.1016/j.stemcr.2016.06.007.

ACKNOWLEDGMENTS

We thank the Biomedicum Stem Cell Center and the Biomedicum Imaging Unit for advice and assistance. We thank Professor Erik Hrabovszky for the generous gift of GnRH antibody, Professor Timo Otonkoski for valuable comments, Mr. Samuel Malone for the human fetus collection and processing of the samples for immunohistochemical procedures, and M.A. Annika Tarkkanen for linguistic guidance. This work was supported by the Academy of Finland, Foundation for Pediatric Research, Sigrid Juselius Foundation, Novo Nordisk Foundation, Emil Aaltonen Foundation, University of Helsinki, Helsinki University Central Hospital, and Agence Nationale de la Recherche, ANR, France (ANR-14-CE12-0015-01 RoSes and GnRH).

Received: November 26, 2015
Revised: June 13, 2016
Accepted: June 15, 2016
Published: July 14, 2016

REFERENCES

Borghese, L., Dolezalova, D., Opitz, T., Haupt, S., Leinhaas, A., Steinfarz, B., Koch, P., Edenhofer, F., Hampl, A., and Brustle, O. (2010). Inhibition of notch signaling in human embryonic stem cell-derived neural stem cells delays G1/S phase transition and accelerates neuronal differentiation in vitro and in vivo. Stem Cells *28*, 955–964.

Casoni, F., Hutchins, B.I., Donohue, D., Fornaro, M., Condie, B.G., and Wray, S. (2012). SDF and GABA interact to regulate axophilic migration of GnRH neurons. J. Cell Sci. *125*, 5015–5025.

Chambers, S.M., Fasano, C.A., Papapetrou, E.P., Tomishima, M., Sadelain, M., and Studer, L. (2009). Highly efficient neural conversion of human ES and iPS cells by dual inhibition of SMAD signaling. Nat. Biotechnol. *27*, 275–280.

Chung, W.C., and Tsai, P.S. (2010). Role of fibroblast growth factor signaling in gonadotropin-releasing hormone neuronal system development. Front. Horm. Res. *39*, 37–50.

Davis, R.P., Casini, S., van den Berg, C.W., Hoekstra, M., Remme, C.A., Dambrot, C., Salvatori, D., Oostwaard, D.W., Wilde, A.A., Bezzina, C.R., et al. (2012). Cardiomyocytes derived from pluripotent stem cells recapitulate electrophysiological characteristics of an overlap syndrome of cardiac sodium channel disease. Circulation *125*, 3079–3091.

Dode, C., Levilliers, J., Dupont, J.M., De Paepe, A., Le Du, N., Soussi-Yanicostas, N., Coimbra, R.S., Delmaghani, S., Compain-Nouaille, S., Baverel, F., et al. (2003). Loss-of-function mutations in FGFR1 cause autosomal dominant Kallmann syndrome. Nat. Genet. *33*, 463–465.

Duggan, C.D., DeMaria, S., Baudhuin, A., Stafford, D., and Ngai, J. (2008). Foxg1 is required for development of the vertebrate olfactory system. J. Neurosci. *28*, 5229–5239.

Falardeau, J., Chung, W.C., Beenken, A., Raivio, T., Plummer, L., Sidis, Y., Jacobson-Dickman, E.E., Eliseenkova, A.V., Ma, J., Dwyer, A., et al. (2008). Decreased FGF8 signaling causes deficiency of gonadotropin-releasing hormone in humans and mice. J. Clin. Invest. *118*, 2822–2831.

Forni, P.E., Taylor-Burds, C., Melvin, V.S., Williams, T., and Wray, S. (2011). Neural crest and ectodermal cells intermix in the nasal placode to give rise to GnRH-1 neurons, sensory neurons, and olfactory ensheathing cells. J. Neurosci. *31*, 6915–6927.

Forni, P.E., Bharti, K., Flannery, E.M., Shimogori, T., and Wray, S. (2013). The indirect role of fibroblast growth factor-8 in defining neurogenic niches of the olfactory/GnRH systems. J. Neurosci. *33*, 19620–19634.

Givens, M.L., Rave-Harel, N., Goonewardena, V.D., Kurotani, R., Berdy, S.E., Swan, C.H., Rubenstein, J.L., Robert, B., and Mellon, P.L. (2005). Developmental regulation of gonadotropin-releasing hormone gene expression by the MSX and DLX homeodomain protein families. J. Biol. Chem. *280*, 19156–19165.

Hay, D.C., Zhao, D., Fletcher, J., Hewitt, Z.A., McLean, D., Urruticoechea-Uriguen, A., Black, J.R., Elcombe, C., Ross, J.A., Wolf, R., and Cui, W. (2008). Efficient differentiation of hepatocytes from human embryonic stem cells exhibiting markers recapitulating liver development in vivo. Stem Cells *26*, 894–902.

Herde, M.K., Iremonger, K.J., Constantin, S., and Herbison, A.E. (2013). GnRH neurons elaborate a long-range projection with shared axonal and dendritic functions. J. Neurosci. *33*, 12689–12697.

Ikeda, K., Ookawara, S., Sato, S., Ando, Z., Kageyama, R., and Kawakami, K. (2007). Six1 is essential for early neurogenesis in the development of olfactory epithelium. Dev. Biol. *311*, 53–68.

Imayoshi, I., Sakamoto, M., Yamaguchi, M., Mori, K., and Kageyama, R. (2010). Essential roles of Notch signaling in maintenance of neural stem cells in developing and adult brains. J. Neurosci. *30*, 3489–3498.

Iyer, A.K., Miller, N.L., Yip, K., Tran, B.H., and Mellon, P.L. (2010). Enhancers of GnRH transcription embedded in an upstream gene use homeodomain proteins to specify hypothalamic expression. Mol. Endocrinol. *24*, 1949–1964.

Kawauchi, S., Shou, J., Santos, R., Hebert, J.M., McConnell, S.K., Mason, I., and Calof, A.L. (2005). FGF8 expression defines a morphogenetic center required for olfactory neurogenesis and nasal cavity development in the mouse. Development *132*, 5211–5223.

Kim, K.H., Patel, L., Tobet, S.A., King, J.C., Rubin, B.S., and Stopa, E.G. (1999). Gonadotropin-releasing hormone immunoreactivity in the adult and fetal human olfactory system. Brain Res. *826*, 220–229.

Kirkeby, A., Grealish, S., Wolf, D.A., Nelander, J., Wood, J., Lundblad, M., Lindvall, O., and Parmar, M. (2012). Generation of regionally specified neural progenitors and functional neurons from human embryonic stem cells under defined conditions. Cell Rep. *1*, 703–714.

Markakis, E.A., Palmer, T.D., Randolph-Moore, L., Rakic, P., and Gage, F.H. (2004). Novel neuronal phenotypes from neural progenitor cells. J. Neurosci. *24*, 2886–2897.

Maroof, A.M., Keros, S., Tyson, J.A., Ying, S.W., Ganat, Y.M., Merkle, F.T., Liu, B., Goulburn, A., Stanley, E.G., Elefanty, A.G., et al. (2013). Directed differentiation and functional maturation of cortical interneurons from human embryonic stem cells. Cell Stem Cell *12*, 559–572.

Merkle, F.T., Maroof, A., Wataya, T., Sasai, Y., Studer, L., Eggan, K., and Schier, A.F. (2015). Generation of neuropeptidergic hypothalamic neurons from human pluripotent stem cells. Development *142*, 633–643.

Merlo, G.R., Mantero, S., Zaghetto, A.A., Peretto, P., Paina, S., and Gozzo, M. (2007). The role of Dlx homeogenes in early development of the olfactory pathway. J. Mol. Histol. *38*, 612–623.

Mikkola, M., Toivonen, S., Tamminen, K., Alfthan, K., Tuuri, T., Satomaa, T., Natunen, J., Saarinen, J., Tiittanen, M., Lampinen, M., et al. (2013). Lectin from *Erythrina cristagalli* supports undifferentiated growth and differentiation of human pluripotent stem cells. Stem Cells Dev. *22*, 707–716.

Miller, A.M., Treloar, H.B., and Greer, C.A. (2010). Composition of the migratory mass during development of the olfactory nerve. J. Comp. Neurol. *518*, 4825–4841.

Noisa, P., Lund, C., Kanduri, K., Lund, R., Lahdesmaki, H., Lahesmaa, R., Lundin, K., Chokechuwattanalert, H., Otonkoski, T., Tuuri, T., and Raivio, T. (2014). Notch signaling regulates the differentiation of neural crest from human pluripotent stem cells. J. Cell Sci. *127*, 2083–2094.

Pankratz, M.T., Li, X.J., Lavaute, T.M., Lyons, E.A., Chen, X., and Zhang, S.C. (2007). Directed neural differentiation of human embryonic stem cells via an obligated primitive anterior stage. Stem Cells *25*, 1511–1520.

Porter, A.G., and Janicke, R.U. (1999). Emerging roles of caspase-3 in apoptosis. Cell Death Differ. *6*, 99–104.

Rawson, N.E., Lischka, F.W., Yee, K.K., Peters, A.Z., Tucker, E.S., Meechan, D.W., Zirlinger, M., Maynard, T.M., Burd, G.B., Dulac, C., et al. (2010). Specific mesenchymal/epithelial induction of olfactory receptor, vomeronasal, and gonadotropin-releasing hormone (GnRH) neurons. Dev. Dyn. *239*, 1723–1738.

Sabado, V., Barraud, P., Baker, C.V.H., and Streit, A. (2012). Specification of GnRH-1 neurons by antagonistic FGF and retinoic acid signaling. Dev. Biol. *362*, 254–262.

Salvi, R., Arsenijevic, Y., Giacomini, M., Rey, J.P., Voirol, M.J., Gaillard, R.C., Risold, P.Y., and Pralong, F. (2009). The fetal hypothalamus has the potential to generate cells with a gonadotropin releasing hormone (GnRH) phenotype. PLoS One *4*, e4392.

Schlosser, G. (2014). Early embryonic specification of vertebrate cranial placodes. Wiley Interdiscip. Rev. Dev. Biol. *3*, 349–363.

Schlosser, G., Awtry, T., Brugmann, S.A., Jensen, E.D., Neilson, K., Ruan, G., Stammler, A., Voelker, D., Yan, B., Zhang, C., et al. (2008). Eya1 and Six1 promote neurogenesis in the cranial placodes in a SoxB1-dependent fashion. Dev. Biol. *320*, 199–214.

Schwanzel-Fukuda, M., and Pfaff, D.W. (1989). Origin of luteinizing hormone-releasing hormone neurons. Nature *338*, 161–164.

Shimamura, K., and Rubenstein, J.L. (1997). Inductive interactions direct early regionalization of the mouse forebrain. Development *124*, 2709–2718.

Simeone, A., Gulisano, M., Acampora, D., Stornaiuolo, A., Rambaldi, M., and Boncinelli, E. (1992). Two vertebrate homeobox genes related to the Drosophila empty spiracles gene are expressed in the embryonic cerebral cortex. EMBO J. *11*, 2541–2550.

Simeone, A., Acampora, D., Pannese, M., D'Esposito, M., Stornaiuolo, A., Gulisano, M., Mallamaci, A., Kastury, K., Druck, T., and Huebner, K. (1994). Cloning and characterization of two members of the vertebrate Dlx gene family. Proc. Natl. Acad. Sci. USA *91*, 2250–2254.

Storm, E.E., Garel, S., Borello, U., Hebert, J.M., Martinez, S., McConnell, S.K., Martin, G.R., and Rubenstein, J.L. (2006). Dose-dependent functions of FGF8 in regulating telencephalic patterning centers. Development *133*, 1831–1844.

Tarozzo, G., Peretto, P., and Fasolo, A. (1995). Cell migration from the olfactory placode and the ontogeny of the neuroendocrine compartments. Zoolog. Sci. *12*, 367–383.

Thomson, J.A., Itskovitz-Eldor, J., Shapiro, S.S., Waknitz, M.A., Swiergiel, J.J., Marshall, V.S., and Jones, J.M. (1998). Embryonic stem cell lines derived from human blastocysts. Science *282*, 1145–1147.

Trokovic, R., Weltner, J., and Otonkoski, T. (2015). Generation of iPSC line HEL24.3 from human neonatal foreskin fibroblasts. Stem Cell Res. *15*, 266–268.

Wang, L., Meece, K., Williams, D.J., Lo, K.A., Zimmer, M., Heinrich, G., Martin Carli, J., Leduc, C.A., Sun, L., Zeltser, L.M., et al. (2015). Differentiation of hypothalamic-like neurons from human pluripotent stem cells. J. Clin. Invest. *125*, 796–808.

Whitlock, K.E., Wolf, C.D., and Boyce, M.L. (2003). Gonadotropin-releasing hormone (GnRH) cells arise from cranial neural crest and adenohypophyseal regions of the neural plate in the zebrafish, *Danio rerio*. Dev. Biol. *257*, 140–152.

Wray, S. (2010). From nose to brain: development of gonadotrophin-releasing hormone-1 neurones. J. Neuroendocrinol *22*, 743–753.

Wray, S., Grant, P., and Gainer, H. (1989a). Evidence that cells expressing luteinizing hormone-releasing hormone mRNA in the mouse are derived from progenitor cells in the olfactory placode. Proc. Natl. Acad. Sci. USA *86*, 8132–8136.

Wray, S., Nieburgs, A., and Elkabes, S. (1989b). Spatiotemporal cell expression of luteinizing hormone-releasing hormone in the prenatal mouse: evidence for an embryonic origin in the olfactory placode. Brain Res. Dev. Brain Res. *46*, 309–318.

Wray, S., Key, S., Qualls, R., and Fueshko, S.M. (1994). A subset of peripherin positive olfactory axons delineates the luteinizing hormone releasing hormone neuronal migratory pathway in developing mouse. Dev. Biol. *166*, 349–354.

Yoon, K., and Gaiano, N. (2005). Notch signaling in the mammalian central nervous system: insights from mouse mutants. Nat. Neurosci. *8*, 709–715.

Zhang, X., Huang, C.T., Chen, J., Pankratz, M.T., Xi, J., Li, J., Yang, Y., Lavaute, T.M., Li, X.J., Ayala, M., et al. (2010). Pax6 is a human neuroectoderm cell fate determinant. Cell Stem Cell *7*, 90–100.

Stem Cell Reports, Volume *7*

Supplemental Information

Development of Gonadotropin-Releasing Hormone-Secreting Neurons from Human Pluripotent Stem Cells

Carina Lund, Kristiina Pulli, Venkatram Yellapragada, Paolo Giacobini, Karolina Lundin, Sanna Vuoristo, Timo Tuuri, Parinya Noisa, and Taneli Raivio

Figure S1 (related to Figure 1)

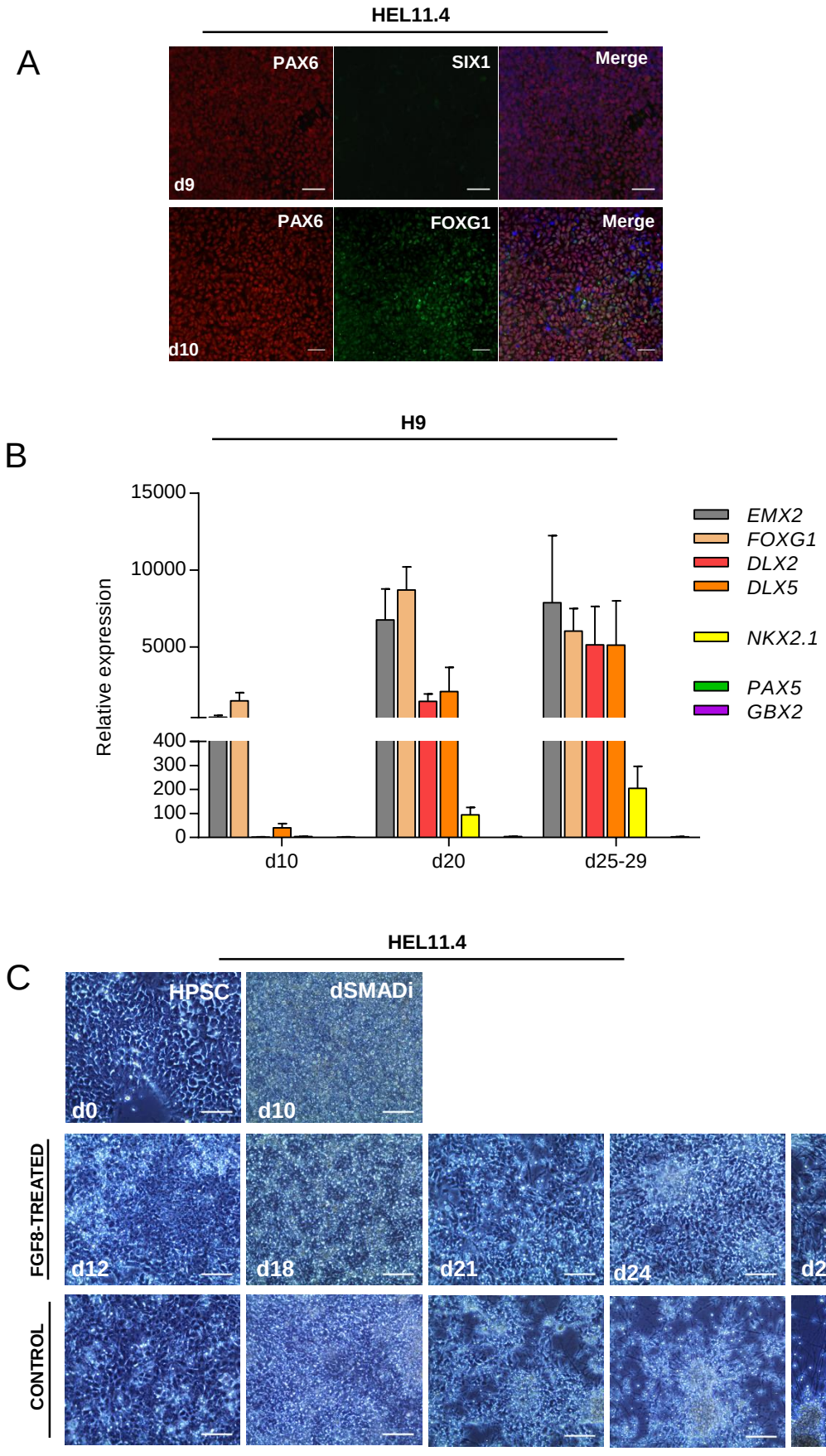

Figure S2 (related to Figure 2)

A

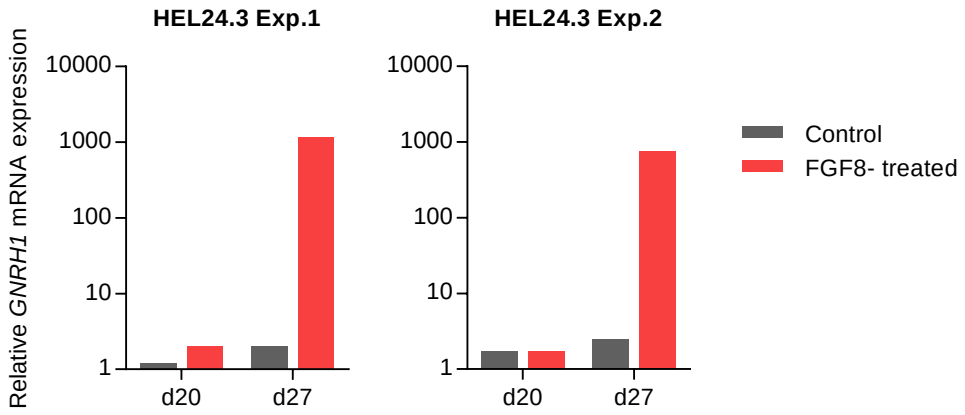

B

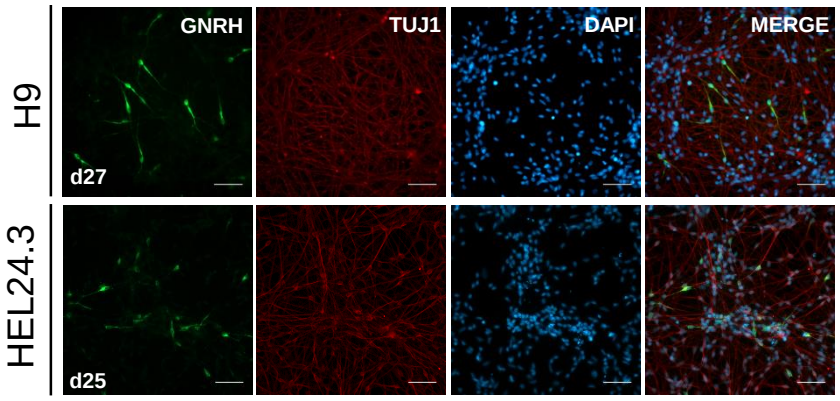

Figure S3 (related to Figure 3)

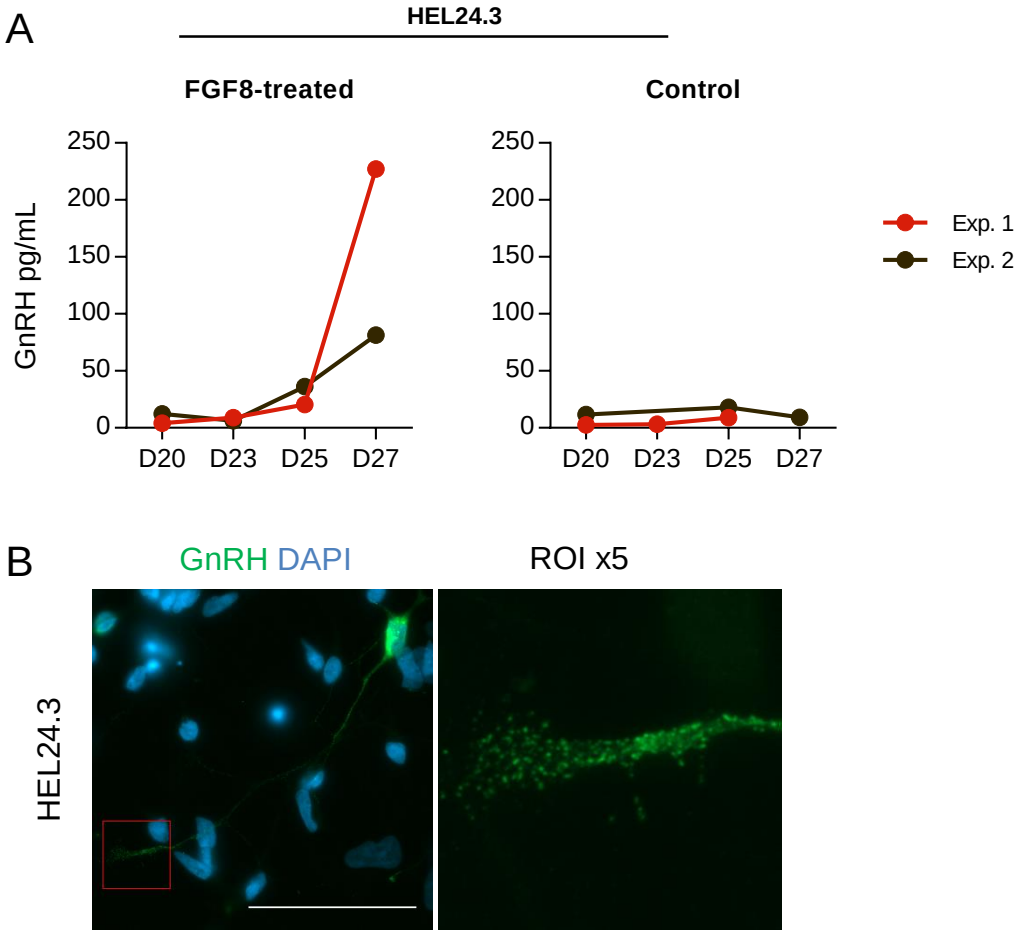

Figure legends

Figure S1. Immunocytochemical characterization after dual SMAD inhibition, and H9-derived cells expression of anterior neural progenitor markers by qPCR during differentiation

A) Immunocytochemistry during the first 10 days of dual SMAD inhibition in HEL11.4-derived cells. PAX6 was detected uniformly throughout the cultures (d9 and 10) and FOXG1 staining was also abundant at d10. In keeping with the qPCR results, expression of preplacodal marker SIX1 was not detected (d9). Scale bar, 50 µm.

B) Relative expression of anterior neural progenitor (*EMX2, FOXG1, DLX2* and *DLX5*), ventral forebrain (*NKX2.1*), and caudal CNS markers (*PAX5* and *GBX2*) at d10, d20 and d25-29 in FGF8-treated H9-derived cells. See Figure 1C for corresponding data from HEL11.4. The relative *FOXG1* expression in H9 cells at d10 appeared higher than in HEL11.4 cells. Bars represent mean + SEM.

C) Representative bright field images (Leica EC3, HiPlan 10x PH objective) of Hel11.4 iPSCs, at specified time points of differentiation. Morphology of FGF8-treated and control cells (CNTRL) are shown. FGF8-treated cells expanded more rapidly as compared to control cells, detectable at days 12, 18 and 24. Scale bar, 100 µm.

Figure S2. GnRH-expressing cells emerge after treatment with FGF8 and DAPT

A) Relative *GNRH1* mRNA expression in HEL24.3 from two individual experiments (See also main Figure 2A).

B) H9-derived, and HEL24.3-derived cells stained by GnRH and TUJ1 at the final stages of differentiation. Scale bar, 50 µm.

Figure S3. GnRH decapeptide secretion in culture medium of FGF8-treated cells.

A) GnRH secretion in HEL24.3 from two experiments, showing increased GnRH secretion in FGF8-treated cells. (See also main Figure 3A).

B) GnRH staining appeared granular, suggesting vesicular packaging of the decapeptide (See also main Figure 3B).

Supplemental Experimental Procedures

Human pluripotent stem cells (hPSCs)

All hPSCs were obtained from intramural Biomedicum Stem Cell Centre core unit (BSCC, University of Helsinki, Finland). HiPSCs HEL11.4 and HEL24.3 were induced at BSCC from healthy donor fibroblasts by Sendai virus cocktail of *OCT4*, *SOX2*, *KLF4* and *C-MYC*. The absence of viral pluripotency factors expression was verified before the onset of differentiation experiments.

All cell culture reagents were purchased from Life Technologies unless stated otherwise. Human embryonic stem cell line H9 (passages 40-50; WiCell) and human induced pluripotent stem cell line HEL11.4 (passages 34-42,(Mikkola et al., 2013)) were maintained on Geltrex®-coated plates with StemPro® (Life technologies) or Essential 8 medium (E8, Life Technologies). hPSCs were passaged by incubating 2-4 minutes in 0.02% EDTA (Sigma) and re-plated at a dilution of 1:4 to 1:6.

Differentiation of hPSCs into neural progenitor cells and GnRH neurons

Cells were maintained throughout the differentiation on Geltrex®-coated plates in N2B27 basal medium (50% DMEM/F12 and 50% Neurobasal medium supplemented with 0.5x N2 and 0.5x B27, 1 mM Glutamax, and 1x Penicillin-Streptomycin (Sigma)). For neural induction, hPSCs were passaged in

StemPro or E8 and re-plated to form a uniform monolayer of cells. When the cells had reached ~95% confluence, medium was replaced with dual SMAD inhibition medium: (N2B27) supplemented with 2 µM Dorsomorphin (BMP inhibitor, Sigma) and 10 µM SB431542 (TGF-β inhibitor, Sigma). On day 10, the cells were dissociated into small clusters by 5 min. incubation with 200 Unit/mL collagenase IV and mechanical scraping, and re-plated at a dilution of 1:2 in dual SMAD inhibition medium supplemented with 10 µM Rock inhibitor Y-27632 (Sigma). At day 11, dual SMAD inhibitors were withdrawn and cells were cultured for 9 days in N2B27 supplemented with 100 ng/mL FGF8 (Peprotech 100-25). On day 20, cells were dissociated with 0.02% EDTA and re-plated at a dilution of 1:6-1:12 in N2B27 with FGF8 to obtain 30-40% confluent layer of small cell clusters. From day 21 onwards, the N2B27 culture medium was supplemented with both 100 ng/mL FGF8 and 20 µM Notch inhibitor DAPT (Sigma). From d0-d21 medium was refreshed daily, and from d21 onwards every 48 hours. Control cells were treated similarly, but without FGF8 supplementation.

RNA extraction, reverse transcription and real-time quantitative PCR

Total RNA was extracted using RNA Spin II kit (Macherey-Nagal) according to the manufacturer's instructions, except that DNase treatment was performed separately with RQ1 DNase (Promega), 1U/µg RNA, in the presence of rRNasin RNase inhibitor (Promega), 1U/µL of reaction volume. First-strand cDNA was reverse-transcribed from 1 µg of total RNA using iScript™ cDNA Synthesis Kit (BIO-RAD). Real-time quantitative PCR reactions included 25 ng of first-strand cDNA, HOT FIREPol® EvaGreen® qPCR Mix Plus (Solis BioDyne), and 0.5 µM forward and reverse primers. Reactions were performed in a LightCycler® 480 (Roche) for 45-50 cycles of 95°C for 15 seconds, 60°C for 20 seconds and 72°C for 20 seconds. The expression levels of target genes were normalized to cyclophilin G. All primer sequences are listed in Table S1.

Immunostainings

Cells were fixed by 4% paraformaldehyde for 10-15 min. at room temperature (RT) and permeabilized in PBS containing 0.5% Triton X-100 (Sigma) for 7 min. Non-specific binding was blocked with UltraVision Protein Block (Thermo scientific) for 10 min. Samples were incubated with primary antibodies overnight at +4°C and with secondary antibodies for 30-45 minutes at RT. Nuclei were counterstained with DAPI (Sigma). Antibodies and DAPI were diluted in PBS containing 0.1% Tween 20 (Sigma). Slides were mounted with Fluoromount^{TM} Aqueous Mounting Medium (Sigma), and images were captured by Zeiss AxioImager.Z1 upright epifluorescence microscopes (Zeiss), or Leica TCS CARS SP8 confocal microscope (Leica) using 20x/NA 0.8, 40x/NA 1.10 and 63x/NA 1.20 HC PL APO CS2 objectives (Biomedicum Imaging Unit), and analyzed with ImageJ (NIH). All antibodies and dilutions used are listed in Table S2.

Quantification of FOXG1 and GnRH positive cells

Quantification of FOXG1 (d21) and GnRH positive cells (d25-29) was based on images taken at 400x magnification (40x objective). Immunopositive cells were counted manually and the relative proportion calculated to the total cell number. Three representative images per experiment were analyzed.

Quantification of secreted GnRH

Cell culture medium was collected concurrently with medium refreshments at indicated time points. Medium was centrifuged shortly and stored in -80°C. Secreted GnRH was quantified by competitive Fluorescent Enzyme Immunoassay (EIA, Phoenix Pharmaceuticals Inc, FEK-040-02) according to manufacturer's instructions, except that undiluted media samples and standard decapeptide (Abcam, ab41769) were diluted in N2B27. GnRH concentrations were determined from the standard curve fitted with four-point parameter logistic nonlinear regression model.

Depolarization by KCl

On d25, the culture medium was refreshed and 16-20 hr later a medium sample was collected. KCl (60 mM) or vehicle (H_2O) was added, the cells were incubated in standard cell culture conditions, and a second medium sample was collected 3 hr later for GnRH analysis with EIA. The experiment was carried out twice in H9 cells and once in HEL11.4 cells. The fold change in GnRH release from KCl-treated over vehicle-treated cells in each experiment was calculated from 2-3 technical replicates.

Gap closure assay

On d20 cells were seeded at high density (1:4 split ratio) onto Geltrex coated 96-well plates containing Oris™ Cell Seeding Stoppers (Platypus Technologies, WI, USA)) to create a 2 mm diameter gap in the middle of the wells. At d25, the stoppers were removed, the cells were washed once with DMEM/F12 to remove unattached cells, and the differentiation media were changed to either N2B27 (Control) or N2B27 and $GABA_A$ receptor agonist muscimol (0.1mM, Sigma) and left to migrate in +37ºC for 50 hrs. At the end of the assay, the cells were fixed and immunostained for GnRH as described above, and the GnRH-positive cells that had entered the uncovered area were counted. Photos of the filled gap area were taken using ZOE™ Fluorescent Cell Imager (BioRad). We counted 2-4 technical replicates (96-wells) per condition per experiment. The assay was carried out four times (twice in H9, and once in HEL11.4 and once in HEL24.3).

Human tissues and immunohistochemistry

A human fetus (8 gestational week) was obtained from voluntarily terminated pregnancy with the parent's written informed consent (Gynecology Hospital Jean de Flandre, Lille, France). Permission to utilize human fetal tissues was obtained from the French agency for biomedical research (Agene de la Biomédecine, Saint-Denis la Plaine, France, protocol n°: PFS16-002). The fetuses were immersion-fixed

in 4% paraformaldehyde in 0.1 M PB (pH 7.4) for 1 week, cryoprotected in 30% sucrose in PBS for 48 hours, embedded in Tissue Tek (Miles, Elkhart, IN), and frozen in liquid nitrogen. Human tissues were cryosectioned (Leica cryostat) at 20 μm. Immunohistochemistry was performed as previously reported (Hanchate et al., 2012). Briefly, the sections were rinsed with 0.1 M PBS and incubated at 4°C overnight with the following primary antisera diluted in 0.1 M PBS containing 0.3% Triton X-100 and 10% normal donkey serum: guinea-pig anti-GnRH (1:10000), a generous gift from Dr. Erik Hrabovszky (Laboratory of Endocrine Neurobiology, Institute of Experimental Medicine of the Hungarian Academy of Sciences, Budapest, Hungary), or rabbit anti-GnRH (1:3000), gift from Prof. G. Tramu (Centre Nationale de la Recherche Scientifique, URA 339, Université Bordeaux I, Talence, France)(Beauvillain and Tramu, 1980), and anti-FOXG1. The sections were then washed in PBS and incubated for 1 hour with Alexa-Fluor 488- and 568-conjugated secondary antibodies (Molecular Probes, Invitrogen, San Diego, CA) diluted 1:400 in PBS and counterstained with DAPI nuclear staining (1:10000; Molecular Probes, Invitrogen, San Diego, CA). Sections were mounted using Mowiol (Calbiochem, USA) and analyzed using a LSM 710 confocal microscope (Zeiss).

Statistical analysis

Statistical analyses to compare GnRH gene expression data between FGF8-treated and control cells, and the number of migrated GnRH neurons between muscimol-treated and control cells was performed using paired, two-tailed t-test of log-transformed expression data (ratio t-test) Prism 5.0 (Graphpad). At least 4 independent experiments were included in each analysis.

Table S1. Primers for real-time qPCR

Symbol	Gene name	Primer sequences
PPIG	Peptidylprolyl isomerase G (Cyclophilin G)	ACTCCCAGCCTGCTTCATAC
		TACGTCTGAAACGATCCCTTG
DLX2	Distal-less homeobox 2	GGCGTTTCCAAAAGACTCA**G**
		GCGGTTCTGGAACCAGATTT
DLX5	Distal-less homeobox 5	CGCTAGCTCCTACCACCAGT
		TTTGCCATTCACCATTCTCA
EMX2	Empty spiracles homeobox 2	GCTTCTAAGGCTGGAACACG
		CCAGCTTCTGCCTTTTGAAC
EYA1	EYA transcriptional coactivator and phosphatase 1	TTTCAACTTGGCAGACACACA
		ATGTGCTTAGGTCCTGTCCG
FOXG1	Forkhead box G1	CCGCACCCGTCAATGACTT
		CCGTCGTAAAACTTGGCAAAG
GBX2	Gastrulation brain homeobox 2	GTTCCCGCCGTCGCTGATGAT
		GCCGGTGTAGACGAAATGGCCG
GNRH1	Gonadotropin-releasing hormone 1	GTCAACTGGCAGAAACCCAA
		TGCCCAGTTTCCTCTTCAAT
NKX2.1	NK2 homeobox 1	AACCAAGCGCATCCAATCTCAAGG
		TGTGCCCAGAGTGAAGTTTGGTCT
PAX6	Paired box 6	TTTGCCCGAGAAAGACTAGC
		CATTTGGCCCTTCGATTAGA
PAX5	Paired box 5	GACACCGTGCCTAGCGTCAG
		GAGCCAGTGGACACTATGCTGTG
SIX1	SIX homeobox 1	TAAGAACCGGAGGCAAAGAG
		AGCAGAAGGACCGAGTTCTG
SOX1	SRY (sex determining region Y) box 1	TCTGTTAACTCACCGGGACC
		ACTCCAGGGTACACACAGGG

Table S2. Antibodies for immunocytochemistry

Antigen	supplier	catalog #	species	dilution
FOXG1	Abcam	ab182659	Rabbit	1:1250
TUJ1	Sigma	T8578	Mouse	1:1000
SIX1	Sigma	SAB2106448	Rabbit	1:500
PAX6	DSHB	AB_528427	Mouse	1:50
MAP2	Neuromics	CH22103	Chicken	1:1000
SOX2	Thermo Scientific	MAI-014	Mouse	1:500
Ki67	Novocastra	NCL-Ki67p	Rabbit	1:500
GnRH	Gift from Erik Hrabovszky	1018	Guinea pig	1:16000
Cleaved caspase-3	Cell signaling	9664	Rabbit	1:200
Secondary antibodies				
anti-rabbit IgG Alexa Fluor 488	Life technologies	A21206	Donkey	1:500
anti-mouse IgG Alexa Fluor 594	Life technologies	A21203	Donkey	1:500
anti-chicken IgG Alexa fluor 546	Thermo Scientific	A11040	Goat	1:500
anti-guinea pig Antibody-CF^{TM}594	Sigma	SAB 4600096	Donkey	1:1000
anti-guinea pig Antibody-CF^{TM}488	Sigma	SAB 4600033	Donkey	1:1000

Supplemental references

Beauvillain, J.C., and Tramu, G. (1980). Immunocytochemical demonstration of LH-RH, somatostatin, and ACTH-like peptide in osmium-postfixed, resin-embedded median eminence. J. Histochem. Cytochem. *28,* 1014-1017.

Hanchate, N.K., Parkash, J., Bellefontaine, N., Mazur, D., Colledge, W.H., d'Anglemont de Tassigny, X., and Prevot, V. (2012). Kisspeptin-GPR54 signaling in mouse NO-synthesizing neurons participates in the hypothalamic control of ovulation. J. Neurosci. *32,* 932-945.

Mikkola, M., Toivonen, S., Tamminen, K., Alfthan, K., Tuuri, T., Satomaa, T., Natunen, J., Saarinen, J., Tiittanen, M., Lampinen, M., *et al.* (2013). Lectin from Erythrina cristagalli supports undifferentiated growth and differentiation of human pluripotent stem cells. Stem Cells Dev. *22,* 707-716.